Microspine-rubber composite for high friction on smooth, rough, and wet surfaces

Constance C. Berdan^{1*}, Bryan G. Johnson², and Elliot W. Hawkes¹

Abstract—As robotic technologies advance and robots move out of factories and labs into the real world, grip on a variety of surfaces (e.g. smooth or rough) in a variety of conditions (e.g. dry or wet) becomes increasingly important. Bioinspired "microspines" have been previously explored, but primarily for vertical climbing applications or for small-scale robots applying low forces (less than 1 N). Further, these works primarily focused on rough surfaces. To advance this area of research, we present a composite material comprising highfriction rubber and compliant nitinol microspines which can passively retract below the surface of the rubber. We show that the composite can support large loads (greater than 75 N) with a high coefficient of friction on both smooth and rough surfaces ($\mu > 1.1$), outperforming microspines alone on smooth surfaces and rubber alone on rough surfaces, especially when wet and oily. Further, due to the retraction of the microspines, the composite does not damage relatively soft, smooth surfaces, like wood flooring. We also test durability, and show that it is improved by microspine compliance, and test the effects of varying microspine diameter, angle, and tip shape. Finally, we demonstrate that a small RC car can climb steeper slopes and stop more quickly in wet conditions with microspines.

I. Introduction

Most terrestrial animals and robots use friction to propel themselves forward across various surfaces, such that a higher coefficient of friction (CoF) allows more aggressive maneuvers with less risk of slip [1]–[3]. While the roughness and condition of the surface impacts the CoF, this is often unable to be controlled, leaving the design of the contact points (e.g., the feet or wheels) as critical to increasing the CoF [4]–[6]. This is particularly the case in wet environmental conditions because the presence of liquids reduces the CoF by coating the asperities (small bumps and pits in the ground surface) [5]–[7]. This makes it harder to successfully navigate inclines and turns, or to stop quickly without skidding [3].

Nature offers design solutions that help improve grip on slippery, rough surfaces. Two prominent mechanisms are tiny hooks or claws for climbing and collapsible microspines for flat surface friction. Various beetles and cockroaches use sharp claws to latch onto asperities, creating large shear forces and even negative normal forces (functionally adhesion), which allow the insects to climb vertical or overhanging rough surfaces [1], [8]. On horizontal surfaces, cockroaches and spiders engage their straight microspines

This work was supported by an Early Career Faculty grant from NASA's Space Technology Research Grants Program.

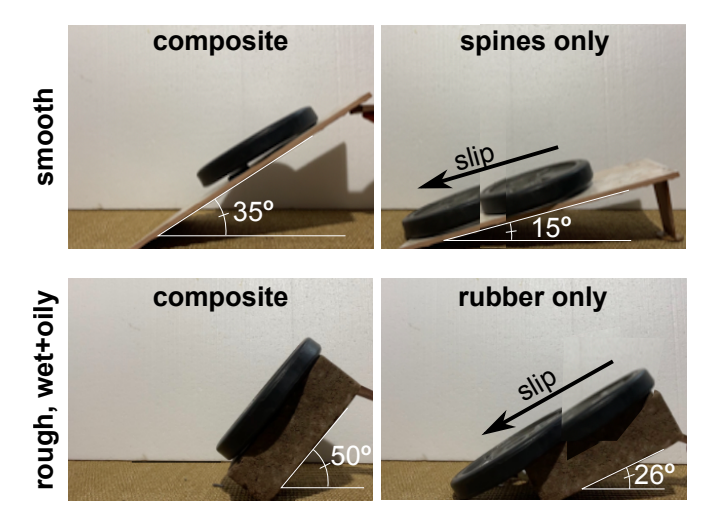


Fig. 1. The microspine-rubber composite outperforms a microspines-only material on a smooth surface (top) and a rubber-only material on a rough, wet, and oily surface (bottom). The mass is 2.2kg.

for improved traction when navigating complex terrain [9], [10]. Experiments with these insects have shown that when moving on rougher surfaces, they impart more lateral force to improve stability while progressing forward. The microspines on cockroach legs are stiff axially to transmit forces when engaged, but easily rotate about their base, enabling them to engage only when necessary [1].

Inspired by the hooks and claws of insects, several mechanisms for climbing robots have been developed [11]–[15]. SpinyBotII uses arrays of sharp, non-deformable hooks (referred to in the literature as microspines) to successfully climb rough surfaces such as concrete [11]. Another larger-scale example is a hand to enable the large robot RoboSimian to climb steep rocky surfaces [16]. These works demonstrate the benefit of multiple steel microspines for load sharing and scaling steep surfaces with high shear forces and little, or even negative, normal force. However, these devices are not designed to support large positive normal forces, which is a requirement for materials used on the feet of large robots designed for locomotion on the ground.

Other work has been bio-inspired by cockroach and cricket leg spines to improve the performance of millirobots during jumping and pulling on mostly flat or inclined surfaces [9], [17]. Using triangular, collapsible microspines attached to the legs, the jumping robot could increase its kinetic energy and jump higher on certain surfaces such as styrofoam, and the microspines enabled the running robot to pull higher loads, run faster, and climb a steeper cork surface incline.

¹Department of Mechanical Engineering, University of California, Santa Barbara, CA 93106.

²Abbott Vascular, Temecula, CA 92591.

^{*} Corresponding author. Email: cberdan@ucsb.edu

Their work predominantly focused on small-scale robots and relatively low forces (for instance VelociRoACH pulled loads lower than 1 N) [9]. At the intersection of these two groups of work is a family of small robots with wheels covered in the hook-type microspine that could roll over flat ground and also climb vertical surfaces [18]. The largest of these robots is 540 g, with most 300 g or less.

Nature provides another solution for improved grip: a hybrid where the hooks that grip rough surfaces are in close proximity with material adapted for grasping smooth surfaces. This is found in both insects [1] and geckos [19], [20]. Few studies have attempted to replicate this ability, and those that have focused on small forces on the order of 1 N. One design required the spines to slip, rotating the foot and enabling a rubber pad to make contact [17], [21]. Another used active Shape Memory Alloy to retract the spines [16].

In this work, we present a microspine-rubber composite. The contributions of our work with respect to previous work are three-fold. First, while most microspine work has focused on low normal force (climbing applications) or low total force (small robots), our composite shows a high coefficient of friction while supporting large normal loads ($\mu > 1.1$, load $> 75\,$ N). Second, we explore the effect of surface condition (dry versus wet and oily) on frictional properties of rubber versus microspines on rough surfaces, a study not currently in the literature. Finally, our composite design with compliant microspines can passively retract below the level of the rubber to enable high friction on smooth surfaces, and does not scratch soft, smooth surfaces, a property not currently addressed in the literature.

What follows is an explanation of the microspine-rubber composite design, simple analytical models of its behavior, a description of its testing methods, and experimental results of the composites's performance.

II. DESIGN CONCEPT

The composite comprises two key elements: a flat surface of high-friction rubber and thin, cylindrical microspines that protrude at an angle through cutouts in the rubber, but are supported only at their bases (Fig. 2A). This allows each cantilevered microspine to easily flex about its base when a load is primarily perpendicular to its axis, yet remain stiff when loaded axially (see Section III). When brought into contact with a rough surface (Fig. 2B, top), the protruding tips of the angled microspines engage with the asperities in the surface to prevent slip. When contacting a smooth surface (Fig. 2B, bottom), the tips of the microspines have no asperities to engage, and the microspines bend until they are flush with the rubber, allowing the rubber to make full contact with the surface (note that rubber is approximately incompressible). At the same time, the flexibility of the microspine allows it bend about its base during a slip event, when the loading angle is beyond what the composite can support (Fig. 2C). This flexing allows graceful failure with minimal damage to the microspine tips.

Parameters of the design, such as microspine diameter and angle, can be chosen to tune performance for specific rough

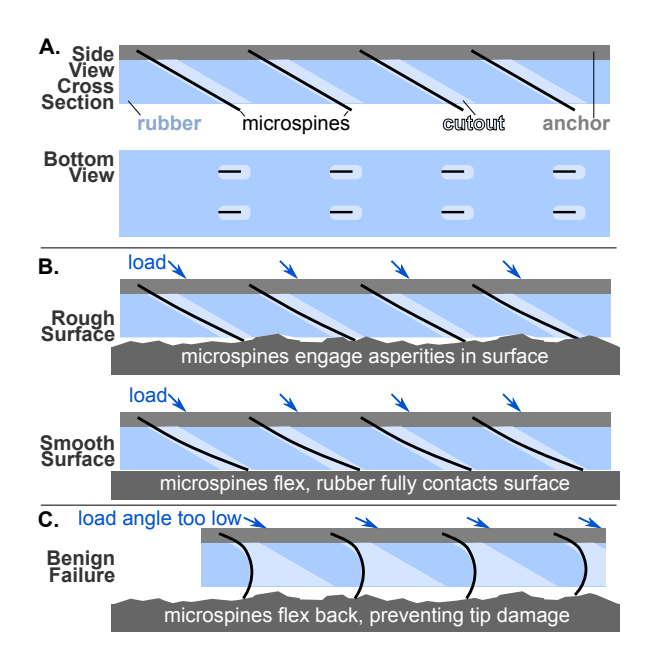


Fig. 2. The design concept of the microspine-rubber composite. A) Microspines are anchored at an angle, pass through cutouts in the rubber, and slightly protruding beyond the surface of the rubber. B) When contacting a rough surface, the microspines flex slightly and find naturally occurring asperities. When contacting a smooth surface, the microspines flex below the rubber, which makes full contact with the surface. C) If the load angle made lower and lower, the composite will eventually slip. In this case, the microspines flex back, preventing damage to the tips and instead dragging the underside of the microspine on the surface.

surfaces. In this work, we focus on concrete and asphalt, and select the appropriate parameters (see Section V). In addition, the basic design presented here can be modified depending on the application. For a rigid robot foot, the design will be very similar to that shown; however, for a pneumatic tire, the anchor is subdivided into sections to give compliance.

III. MODELING

The basic model of how a microspine works is covered in previous literature (e.g., [11], [16]). To summarize, the local surface normal does not match the global surface normal when roughness and asperities exist (see Fig. 2B). Locally, there are sections where the surface is nearly perpendicular to the microspine tip, meaning that a relatively low local CoF results in a much higher functional global CoF. A high global CoF means the material can support shallow loading angles, as measured from the surface, approaching a pure shear load. This means any load from pure normal to shallow, near-shear will be supported without slip. In the remainder of this section, we present simple models for predicting the trends of the behavior of our microspine-rubber composite.

A. Ideal Microspine Angle and Diameter Models

We predict that for a given surface texture, there should be an ideal angle at which the microspine should be mounted with respect to the anchor, with higher and lower mounting angles resulting in lower performance (i.e., lower CoF and less shallow loading angle, measured from the surface). This is because there are two competing effects, one decreasing

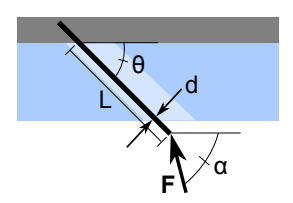


Fig. 3. Geometry and variables for modeling.

CoF and the other increasing CoF, with mounting angle. The first effect is that straight microspines will deform due to high stress at the base, and bend and slip if the loading angle, α , is much shallower than their mounting angle, θ (Fig. 3). The maximum stress, σ_m , at the base of a microspine due to this non-axial loading can be written as

$$\sigma_m = \frac{Mc}{I} = \frac{32FL\sin(\theta - \alpha)}{\pi d^3},\tag{1}$$

where M is the moment about the base, c is the distance from the neutral axis to the edge of the microspine, I is the moment of inertia for the circular cross-section, F is the load, L is the unsupported length, and d is the diameter. The stress grows roughly linearly with the difference in loading versus mounting angle for small angular differences. In Section V-A, we calculate the expected limit to loading angle for our microspine geometry.

At the same time, it is not possible to simply decrease the mounting angle to zero to allow very shallow loading angles because of a second competing effect: microspines with a low mounting angle cannot reach deep into a rough surface to engage with asperities; they will only skim the surface. Thus, we predict to find an optimal angle that is large enough to allow the microspine to reach into asperities, but shallow enough to remain within the stress limit of the microspine.

Similarly, we expect two competing effects for spine diameter: too large of a diameter and the microspine will not be able to reach into asperities, while too small of a diameter will not support the loads without buckling or bending. We test these predictions in Section V-A.

B. Wet Rough Surface Slip Model

We predict that regardless of surface condition (wet and oily or dry), the slip angle should vary little for our composite on rough surfaces. This is because, as described above, the global CoF is a result of the local interactions of all of the microspines. If many of the microspines have nearly perpendicular contact with the local surface, then they will not slip whether dry (high local CoF) or wet and oily (low local CoF). Instead, failure will likely be dictated by stress overload at the microspine base, as described in the previous section. We test this prediction in Section V-B.

C. Smooth Surface Slip Model

We predict that the performance of the composite will be nearly equivalent to that of rubber on smooth surfaces, beyond a critical load. This is because beyond the critical load, the microspines will bend enough to allow the rubber to fully contact the surface, and the total effective CoF, μ_{eff} , will approach the rubber CoF, μ_r :

$$\mu_{eff} = \frac{F_{N,r}\mu_r}{F_N} + \frac{F_{N,s}\mu_s}{F_N},$$
 (2)

where $F_{N,r}$ and $F_{N,s}$ are the portions of the normal load on the rubber and microspines, respectively, and μ_s is the local CoF of the microspine on the surface. Further, we can write

$$F_{N,s} = \frac{3\delta EI}{L^3 \cos \theta} \text{ and }$$
 (3)

$$F_{N,r} = F_N - F_{N,s}$$
, for $F_N > F_{N,s}$, else $F_{N,r} = 0$, (4)

where δ is the deflection of the microspine toward the rubber and E is the elastic modulus of the microspine. Therefore, for low normal loads ($F_N < F_{N,s}$), there will be no normal load on the rubber, and the effective CoF will equal the CoF of the microspine (relatively low—metal on a hard smooth surface). However, at very high normal loads, the effective CoF will approach that of the rubber, since $F_{N,s}$ will saturate (δ will not increase) once the rubber contacts the surface (assuming the rubber deforms little compared to the motion of the tip of the microspine). We test this prediction in Section V-C.

IV. METHODS

A. Material Choices

For the rubber of the composite, we chose a high-friction, long-wearing graphene-doped synthetic tire rubber (Vittoria). For the microspines, we chose nickel-titanium alloy (nitinol), because of its ability to yield but recover elastically [22]. As mentioned in Section III-B, the primary failure mode for the composite slipping on a rough surface is backward bending of the microspines about their base after the yield stress is reached. While steel would plastically deform after yielding, nitinol will recover elastically. It is also relatively wear-resistant [23], [24].

B. Microspine-rubber Composite Test Samples

In order to assess the benefit of adding microspines to the base of various robot feet, we designed various test samples to emulate different foot geometry. The three designs are a hard, flat sample, a hard spherical sample, and soft tire. The flat sample is a rectangle with sides of $(3.175\,\mathrm{cm}\times3.000\,\mathrm{cm})$ and is made of 3D-printed PLA plastic with three microspines arranged in a triangle pattern (1 spine per 3.175 square centimeters). (Fig. 4). The spherical sample is also made from 3D-printed PLA plastic, with a diameter of 4.4 cm, and 6 spines per square centimeter.

The tire is from an RC car and has a outside diameter of 14.1 cm and 4 spines per square centimeter. The anchor



Fig. 4. A) Side view of microspine-rubber composite in flat sample. B) A toothpick is strong enough to deform a flexible microspine into the surface of the rubber.

for the microspines was fabricated from carbon fiber and embedded inside the tire. All spines protruded the same length from the treads and angled normal from the tire.

The flat sample was used for ideal diameter testing, in which the nitinol microspines were varied in diameter from 0.5 mm to 2.0 mm, in both a square-cut condition (perpendicular cut at the tip) and sharpened condition (angled cut at the tip). The flat sample was also used for ideal angle testing, in which the mounting angle was varied from 15° to 60° by 15° increments (with 0.64 mm diameter, square-cut microspines). A final sample was created by embedding microspines with carbon fiber anchors into the forefoot of the soles (7.5 cm x 5 cm) of running shoes (Nike Pegasus).

C. Slip Angle Testing Procedures

Rough surface slip testing was done on a solid block of cast concrete (39.7 cm \times 14.0 cm \times 7.3 cm). The wet condition was created by adding a small amount of vegetable oil (Crisco Canola) spread uniformly over the surface. Smooth surface testing was done on ceramic tile (30.0 cm x 11.7 cm x 0.9 cm (Carrara)). We test only dry smooth surfaces, as the effect of water and oil on rubber performance is well studied (e.g. [5], [6]). Each surface was supported at an angle, and each test sample was mounted to a rigid sample holder (3Dprinted with PLA). A vertical force of approximately 75 N was applied to the back of the sample holder via a metal rod of diameter 0.7 cm and length 25.4 cm. The smooth test surface was also tested with no mass on the sample (the sample has a mass of 10 g) and with a 0.96 N force, to explore the effect of varied load. Testing began at a steep loading angle (between the surface and the vertical), and incremented by approximately 2° for each test until a slip occurred. A slip is defined as when the sample overcomes the static friction force to slide down the surface. This was repeated three times for each condition. The CoF was calculated as the arctangent of the maximum loading angle. We calculated only one direction for the CoF because our spine angling. If we rotated the spines 180°, then the friction would behave like rubber only because the spines would deform since our samples are designed for forward travel. Omnidirectional friction can be obtained by making the spines angled in all directions.

D. Durability and Surface Damage Testing Procedures

To test the durability of the microspine-rubber composite, we forced it to slip on the rough concrete surface. This sample had 0.64 mm diameter microspines at a 45° mounting angle. We also tested a sample with the same microspine diameter and mounting angle but with a shorter length of unsupported microspine beyond the anchor (2.2 mm as opposed to 5.8 mm in the standard sample). The microspines in this sample are limited in their ability to flex backward during failure, potentially wearing more quickly. The samples were made to slip in sets of 10, tested, slipped 10 more times, and repeated for a total of 100 slips. We only tested and measured the wear of these two samples, and future work could explore if variables such as mounting angle and

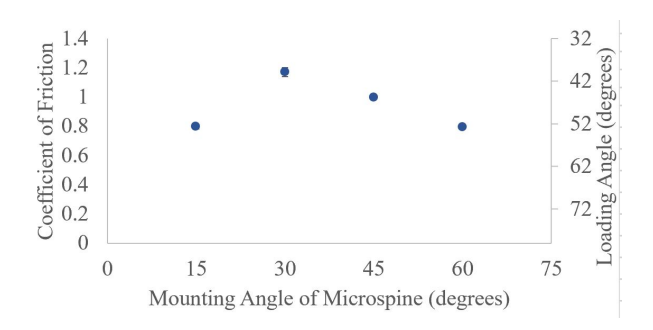


Fig. 5. Results for the ideal microspine angle tests on rough dry concrete. Tests were done with the 0.64 mm nitinol at 15°, 30°, 45°, and 60° angles.

diameter affect durability. Additionally, as a demonstration of the durability technology, we tested the running shoe sample by measuring slip angle before and after outdoor running sessions. Each session included running 16 km at $3.8 \, {\rm m \, s^{-1}}$, equalling roughly 6,000 steps per shoe, and applying over $1300 \, {\rm N}$, or twice the bodyweight of a $68 \, {\rm kg}$ runner. A total of four sessions were completed.

To test the damage that the microspine-rubber composite causes to a smooth, soft surface, the composite was made to slip on an engineered wood surface (Bruce, Engineered Red Oak Flooring) using the same samples in the previous test.

E. RC Car Testing Procedures

Done as a demonstration of the microspine performance, 0.64 mm diameter microspines were inserted into the front tires of an RC car (Mainan). The car was driven down a stretch of road until it had reached maximum cruising speed (approximately 0.725 ms⁻¹) and near-constant velocity, then abruptly braked by reversing the motor. The distance it skidded before coming to a stop was recorded. For this test, the wet condition was done just after the rain on an asphalt street (the pavement was wet but not puddled, and oil was present from usual car use). Ten trials were done instead of three due to the higher standard deviation of the data.

V. RESULTS

A. Ideal Microspine Angle and Diameter Results

The simple model from Section III-A predicts that the CoF will be maximized for an intermediate microspine mounting angle. The results from our tests show this trend, with a mounting angle of 30° producing the largest values of CoF, for tests on both dry and wet and oily rough surfaces. The data for the dry tests are shown in Fig. 5. As predicted, for high mounting angles (45° and 60°), the lowest achievable loading angle was equal to or slightly lower than the spine mounting angle. The 60° microspine slipped at a loading angle of 52°, while the 45° microspine slipped at 45°. Also as predicted, at low mounting angles (15° and 30°), the lowest loading angle did not reach as low as the mounting angle (40° for the 30° mounting and 52° for the 15° mounting).

We also tested how varying diameter and tip shape (square-cut versus sharpened) of the microspine affected performance on dry and wet and oily rough surfaces. As

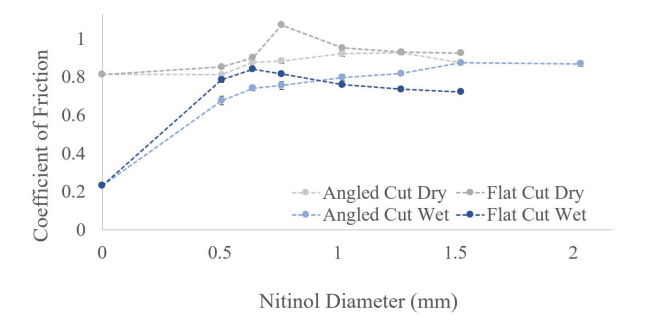


Fig. 6. Results for the ideal diameter tests. Tests included microspines ranging from 0.5 mm to 2.0 mm. Both tip conditions (square-cut and sharpened) were tested in dry and wet conditions.

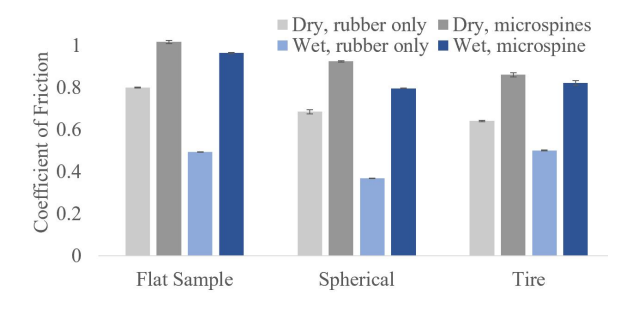


Fig. 7. Results of testing flat, spherical and tire samples on dry and wet rough surfaces. For each, a rubber-only sample is compared to the microspine-rubber composite.

shown in Fig. 6, the square-cut microspines show a maximum at 0.64 mm for wet and 0.76 mm for dry. In contrast, the sharpened microspines did not show a clear maximum in the range tested. However, sharpened microspines are impractical because they dull quickly with use.

B. Rough Surface Results

The model from Section III-B suggests that the CoF of the microspine-rubber composite should not be substantially different on dry versus wet rough surfaces, unlike standard rubber. This trend is indeed shown by the data in Fig. 7. Across the three test sample types (flat, spherical, and tire), the CoF for the rubber decreases noticeably from dry to wet, while the CoF for the microspine-rubber composite decreases only slightly (and remains higher than that of even the dry rubber case). Not shown are results for microspine-only samples on wet and dry rough surfaces; these samples had the same CoFs as those of the composite, showing that the addition of rubber to form the composite did not sacrifice performance on rough surfaces.

C. Smooth Surface Results

The modeling of Section III-C predicts that the microspine-rubber composite will perform similarly to a rubber-only sample on smooth dry surfaces at high load, but less well at very small loads that are too small to retract the microspines. The data shown in Fig. 8 confirms this prediction, showing a relatively low CoF for the microspine-rubber composite for loads under 1 N, but a CoF that is comparable to the rubber-only case at a slightly higher

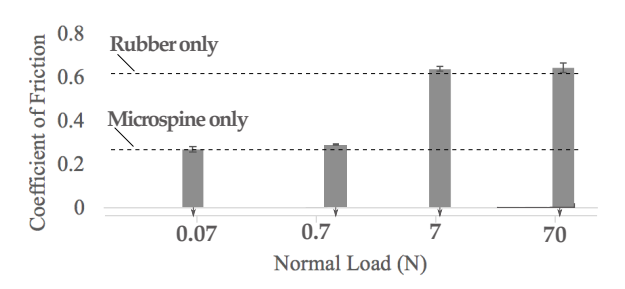


Fig. 8. Results for samples tested on a smooth dry surface. At very low normal loads, the composite does not perform as well as rubber, because the microspine do not retract, but at slightly higher loads (> 1 N), the composite performs as well as the rubber-only sample (and much better than the microspines-only sample).

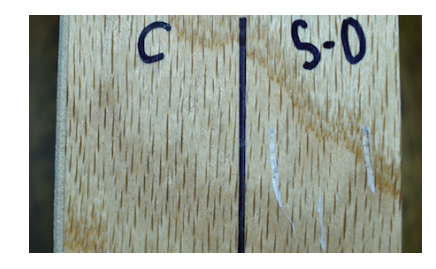


Fig. 9. Image showing wood floor board after failure of the composite ("C", left) versus a microspines-only sample ("S-O", right). There is no visible damage for the composite. The microspine scratches are 0.5 mm deep.

load of 7 N; additional load does not measurably affect performance. Further, the microspine-only sample performs much worse than the rubber-only and the composite, as it only has metal contacting the smooth surface. We also tested damage on a soft smooth surface, and qualitative results show significant damage with microspines only, but no visible damage with the composite (Fig. 9).

D. Durability Results

For flat samples made to intentionally fail repeatedly, we see that the flexible microspines of the composite design show little performance degradation, while short, stiff microspines lose approximately 25% of their peak CoF value after 100 failure events (Fig. 10). For the running shoe durability testing results (not shown), we found that the CoF did not deteriorate for the first three running sessions (total of 48 km or approximately 18,000 steps, each with a load of over 1300 N), while a small, but measurable decrease in CoF (approximately 10%) was seen after the fourth session.

E. RC Car Results

Finally, the results of testing the RC car on an outdoor asphalt road showed measurable improvements in distance to stop (Fig. 11). While improvements were visible in a dry test, the more dramatic improvement occurred on the wet road, where the car with microspines halved the stopping distance. The microspines also improved steep incline performance (see attached Video).

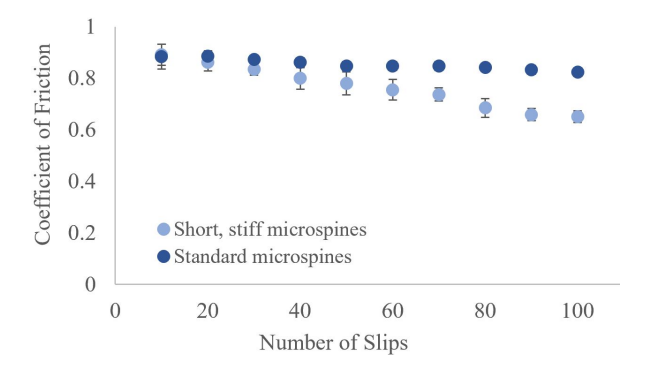


Fig. 10. Results comparing the changing CoF with use. When the microspines can deform into the rubber, their performance remains consistent with use.

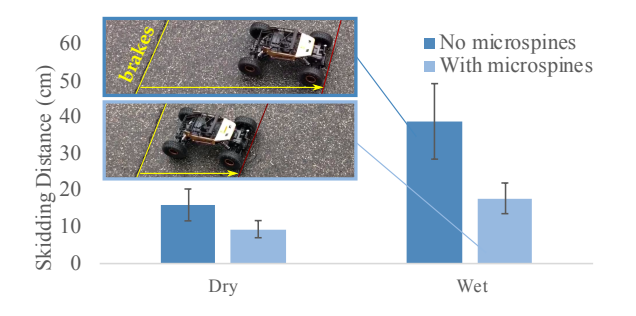


Fig. 11. Results demonstrating the performance of the microspines when embedded in the tires of an RC car. Testing was done for both dry and wet conditions with 0.64 mm flat cut microspines.

VI. DISCUSSION

Section V presents a variety of results confirming the predicted trends for the behavior of the microspine-rubber composite and demonstrating performance benefits compared to either rubber-only or microspines-only materials. Our results suggest that the composite could work on a wide range of robotic morphologies, including flat feet, spherical or hemispherical feet, and wheeled tires—covering much of the literature. A limitation of the study is that it did not directly test tank treads (found on some robots); however, similar performance to the flat samples might be expected. The results also demonstrate increased CoF under high normal loads, filling a gap in the microspine literature. We used 75 N for slip tests on 9 cm² samples for greater than 80 kPa of pressure, and 1300 N on the forefoot of the shoe with area 38 cm² for greater than 340 kPa of pressure.

We also showed that there is an ideal diameter and mounting angle of the microspine within the ranges tested. However, the exact values of these likely depend on the size, shape, and density of asperities. Since this study was limited to two common rough surfaces (concrete and asphalt), further studies would help improve our understanding of how surface morphology affects ideal diameter and mounting angle.

Wear is a common concern in most foot and tire designs, and is of even greater concern for a microspine design, since a relatively sharp tip is required. However, our durability testing suggests that the composite with flexible microspines

is more durable than a stiff-spine design and shows minimal performance decay across 100 simulated failures. We note that during normal uses, such a catastrophic sliding failure would rarely, and hopefully never, occur. Accordingly, we also tested thousands of loading cycles without catastrophic slip with the composite embedded into the sole of a running shoe. Only after 24,000 loading cycles were we able to measure a small deterioration in performance. We believe that part of this high durability is due to using square-cut microspines, rather than sharpened ones. The microspines cannot become duller than they are when manufactured; the eventual decay in performance is likely due to complete removal of the end of the microspine, making it eventually too short to reach into asperities. However, the ability to take enough steps to cover greater than the distance of a marathon with our preliminary design is promising. Further testing could examine the durability for wheeled designs.

The composite design also demonstrated an ability to handle rough and smooth surfaces well, overcoming the shortcomings of both a microspine-only or rubber-only design. The compliance of the microspines in our hybrid composite design allows them to deform under small loads when contacting smooth surfaces. This means that a large load will not be applied through the microspine to a smooth surface, preventing damage to soft, smooth surfaces. This is a key characteristic for a foot or wheel material that might need to work both indoors and outdoors.

Finally, our RC car results showed that the benefits of the microspine-rubber composite are not limited to static situations. This car recorded being able to climb steeper inclines and a stop after a shorter braking distance with the addition of the microspines into its tires. As mentioned earlier, the microspines were only embedded into the front two tires, so we would anticipate higher changes in CoF if all four tires had microspines.

VII. CONCLUSION

We present a microspine-rubber composite for increasing the CoF of robot feet and wheels in contact with various realworld surfaces. We introduced the design, derived simple models of its behavior, and presented results verifying the trends predicted by the models as well as showing the limits of composite's performance. Our work helps advance the literature on microspines with three primary contributions. First, we present a microspine design that supports large normal loads (on the order of 10 N to 1000 N). Second, we present data exploring the difference in microspine behavior on dry versus wet rough surfaces. Third, our composite design features compliant microspines that passively retract, enabling high CoF on both rough and smooth surfaces without damaging them and demonstrating performance for over ten thousand cycles. Future work will explore more surfaces as well as integrate the composite into various robotic systems to test in real-world robot use cases.

ACKNOWLEDGMENT

The authors thank all members of the Hawkes Lab for various aid. C.C.B. also thanks A. Pedersen and N. Lysek at UCSB for their help with videos and formatting.

REFERENCES

- [1] Z. Dai, S. N. Gorb, and U. Schwarz, "Roughness-dependent friction force of the tarsal claw system in the beetle Pachnoda marginata (Coleoptera, Scarabaeidae)," *Journal of Experimental Biology*, vol. 205, no. 16, pp. 2479–2488, 2002.
- [2] Y. Chen, K.-j. Wang, and W.-f. Zhou, "Evaluation of surface textures and skid resistance of pervious concrete pavement," *Journal of Central South University*, vol. 20, no. 2, pp. 520–527, Feb. 2013.
- [3] S. M. Kamal Hossain, D. Liping Fu, and B. Law, "Winter Contaminants of Parking Lots and Sidewalks: Friction Characteristics and Slipping Risks," *Journal of Cold Regions Engineering*, vol. 29, no. 4, p. 04014018, Dec. 2015.
- [4] P. M. Santos and E. N. Júlio, "A state-of-the-art review on roughness quantification methods for concrete surfaces," *Construction and Building Materials*, vol. 38, pp. 912–923, Jan. 2013.
- [5] D. P. Manning, C. Jones, F. J. Rowland, and M. Roff, "The Surface Roughness of a Rubber Soling Material Determines the Coefficient of Friction on Water-Lubricated Surfaces," *Journal of Safety Research*, vol. 29, no. 4, pp. 275–283, Dec. 1998.
- [6] I.-J. Kim, H. Hsiao, and P. Simeonov, "Functional levels of floor surface roughness for the prevention of slips and falls: Clean-anddry and soapsuds-covered wet surfaces," *Applied Ergonomics*, vol. 44, no. 1, pp. 58–64, Jan. 2013.
- [7] Q. Zeng and G. Dong, "Influence of Load and Sliding Speed on Super-Low Friction of Nitinol 60 Alloy under Castor Oil Lubrication," *Tribology Letters*, vol. 52, no. 1, pp. 47–55, Oct. 2013.
- [8] M. O. Tokhi and G. S. Virk, Advances in Cooperative Robotics: Proceedings of the 19th International Conference on CLAWAR 2016. WORLD SCIENTIFIC, Sep. 2016.
- [9] J. S. Lee and R. S. Fearing, "Anisotropic collapsible leg spines for increased millirobot traction," in 2015 IEEE International Conference on Robotics and Automation (ICRA). Seattle, WA, USA: IEEE, May 2015, pp. 4547–4553.
- [10] K. A. Daltorio, T. E. Wei, A. D. Horchler, L. Southard, G. D. Wile, R. D. Quinn, S. N. Gorb, and R. E. Ritzmann, "Mini-Whegs TM Climbs Steep Surfaces Using Insect-inspired Attachment Mechanisms," *The International Journal of Robotics Research*, vol. 28, no. 2, pp. 285–302, Feb. 2009.
- [11] A. T. Asbeck, S. Kim, M. R. Cutkosky, W. R. Provancher, and M. Lanzetta, "Scaling Hard Vertical Surfaces with Compliant Microspine Arrays," *The International Journal of Robotics Research*, vol. 25, no. 12, pp. 1165–1179, Dec. 2006.
- [12] S. Wang, H. Jiang, T. Myung Huh, D. Sun, W. Ruotolo, M. Miller, W. R. T. Roderick, H. S. Stuart, and M. R. Cutkosky, "SpinyHand: Contact Load Sharing for a Human-Scale Climbing Robot," *Journal of Mechanisms and Robotics*, vol. 11, no. 3, p. 031009, Jun. 2019.
- [13] S. Wang, H. Jiang, and M. R. Cutkosky, "Design and modeling of linearly-constrained compliant spines for human-scale locomotion on rocky surfaces," *The International Journal of Robotics Research*, vol. 36, no. 9, pp. 985–999, Aug. 2017.
- [14] ——, "A palm for a rock climbing robot based on dense arrays of micro-spines," in 2016 IEEE/RSJ International Conference on Intelligent Robots and Systems (IROS). Daejeon, South Korea: IEEE, Oct. 2016, pp. 52–59.
- [15] M. J. Spenko, G. C. Haynes, J. A. Saunders, M. R. Cutkosky, A. A. Rizzi, R. J. Full, and D. E. Koditschek, "Biologically inspired climbing with a hexapedal robot," *Journal of Field Robotics*, vol. 25, no. 4-5, pp. 223–242, Apr. 2008.
- [16] W. Ruotolo, F. S. Roig, and M. R. Cutkosky, "Load-Sharing in Soft and Spiny Paws for a Large Climbing Robot," *IEEE Robotics and Automation Letters*, vol. 4, no. 2, pp. 1439–1446, Apr. 2019.
- [17] J. S. Lee, "Increased Millirobot Traction in Running and Jumping through Leg Spines," pp. 1–69, 2018.
- [18] K. Carpenter, N. Wiltsie, and A. Parness, "Rotary Microspine Rough Surface Mobility," *IEEE/ASME Transactions on Mechatronics*, vol. 21, no. 5, pp. 2378–2390, Oct. 2016.
- [19] K. Autumn, "How Gecko Toes Stick," American Scientist, vol. 94, no. 2, p. 124, 2006.

- [20] Y. Tian, N. Pesika, H. Zeng, K. Rosenberg, B. Zhao, P. McGuiggan, K. Autumn, and J. Israelachvili, "Adhesion and friction in gecko toe attachment and detachment," *Proceedings of the National Academy of Sciences*, vol. 103, no. 51, pp. 19320–19325, Dec. 2006.
- [21] J. S. Lee, M. Plecnik, J.-H. Yang, and R. S. Fearing, "Self-Engaging Spined Gripper with Dynamic Penetration and Release for Steep Jumps," in 2018 IEEE International Conference on Robotics and Automation (ICRA). Brisbane, QLD: IEEE, May 2018, pp. 1–8.
- [22] S. W. Robertson, A. R. Pelton, and R. O. Ritchie, "Mechanical fatigue and fracture of Nitinol," *International Materials Reviews*, vol. 57, no. 1, pp. 1–37, Jan. 2012.
- [23] W. Chrzanowski, E. A. A. Neel, D. A. Armitage, K. Lee, W. Walke, and J. C. Knowles, "Nanomechanical evaluation of nickel-titanium surface properties after alkali and electrochemical treatments," *Journal of The Royal Society Interface*, vol. 5, no. 26, pp. 1009–1022, Sep. 2008
- [24] R. Neupane and Z. Farhat, "Wear mechanisms of nitinol under reciprocating sliding contact," Wear, vol. 315, no. 1-2, pp. 25–30, Jul. 2014